J. Synchrotron Rad. (1995). **2**, 143–147

Long Horizontal Parallel Slits with 0.03° Angular Resolution for Powder Diffraction Using Synchrotron Radiation

H. Toraya,[a] M. Takata,[b] H. Hibino,[a] J. Yoshino[a] and K. Ohsumi[c]

[a]Ceramics Research Laboratory, Nagoya Institute of Technology, Asahigaoka, Tajimi 507, Japan, [b]Department of Applied Physics, Faculty of Engineering, Chikusa-ku, Nagoya 464-01, Japan, and [c]Photon Factory, High-Energy Physics Laboratory, Oho, Tsukuba 305, Japan

(Received 10 January 1995; accepted 16 February 1995)

Long horizontal parallel slits with angular apertures of 0.032 and 0.065° were constructed for powder diffraction experiments with synchrotron radiation. They have been tested at the BL-4B experimental station at the Photon Factory by using a monochromatized beam with a wavelength of 1.528 Å. The horizontal parallel slits with the smaller aperture gave a full-width at half-maximum of 0.030 (1)° for the (200) reflection from CeO_2 and an intensity about one order of magnitude higher than that obtained with a receiving slit in the same angular resolution, demonstrating the finest horizontal parallel slits developed so far. The misalignment of the horizontal parallel slits does not affect the intensity whilst it shifts the Bragg-peak positions systematically.

Keywords: parallel slits; beam collimation; powder diffraction.

1. Introduction

Parallel-beam optics using synchrotron radiation become very advantageous for high-resolution powder diffraction experiments. Such optics can be most effectively used in combination with either horizontal parallel slits or crystal analyzers mounted on the diffracted beam side. Horizontal parallel slits consist of a number of long thin foils stacked parallel at very narrow spacing, whilst the crystal analyzer usually uses flat perfect crystals or channel-cut crystals such as Si or Ge. In parallel-beam optics, these analyzers can eliminate the shift in the Bragg-peak positions arising from specimen-displacement- and specimen-transparency-type aberrations, which are inevitable in the use of conventional receiving slits (Hastings, Thomlinson & Cox, 1984). The crystal analyzer generally gives higher angular resolution of 0.01–0.05° (Cox, 1992), whilst the horizontal parallel slits are advantageous in obtaining high intensity.

The use of horizontal parallel slits for powder diffraction experiments with synchrotron radiation was first reported by Parrish, Hart, Erickson, Masciocchi & Huang (1986) and Hart & Parrish (1986). These horizontal parallel slits were 100 mm in length with a 0.17° angular aperture. Longer horizontal parallel slits (365 mm) with higher angular resolution (0.05° angular aperture) were further developed by Parrish & Hart (1987) and have been used at Stanford Synchrotron Radiation Laboratory (SSRL). Horizontal parallel slits based on the optics design developed at SSRL were constructed at Daresbury Laboratory (355 mm length, 0.069° angular aperture) (Cernik, Murray, Pattison & Fitch, 1990). Some were also constructed at the Photon Factory by Ohno, Harada, Yamagata & Yamazaki (1991) (0.057° angular aperture, 100 mm length) and recently by Takata, Kisono, Sakata & Sasaki (1993) (0.038 and 0.076° angular apertures, 300 mm length). The horizontal parallel slits have another advantage in that an arbitrary angular resolution can be chosen by selecting the foil length and the spacing between the foils (Hart, 1991). High precision of assembly is, however, required in constructing the horizontal parallel slits because long flat foils must be stacked parallel at spacings of 0.1–0.2 mm to a certain height. Therefore, a limit in the angular resolution of the horizontal parallel slits results from the technical difficulty of stacking the foils. However, it has been suggested that very long horizontal parallel slits with 0.02° resolution could be made in principle (Parrish, Hart & Toraya, 1990).

The present study was conducted as part of research and development for SPring-8 (a new synchrotron radiation light source under construction in Nishi-Harima, Japan). It has two main purposes. One is to achieve 0.03° angular resolution and the other is to stack the foils to a height of 25 mm, which is required for asymmetric 2θ scanning at a fixed incident angle (Toraya, Huang & Wu, 1993).

2. Instrumentation

Two sets of horizontal parallel slits with different angular apertures were constructed by Rigaku Corporation. They are hereafter called HPS1 and HPS2 for horizontal parallel slits with smaller and larger apertures, respectively. Selected specifications are given in Table 1. A vertical parallel slit with an angular aperture of 1° for suppressing the axial divergence was also made.

The powder diffractometer (PFPD) installed at the BL-4B experimental station at the Photon Factory (Uno *et al.*, 1988) was used for testing the horizontal parallel slits. It is situated 20 m away from a bending-magnet light source and

Table 1
Selected specifications for the horizontal parallel slits.

	HPS1	HPS2
Angular aperture (°)	0.032	0.065
Transmission efficiency (%)	67	80
Spacing between the two foils (mm)	0.1	0.2
Number of foils	167	100
Foil material	Stainless steel	
Foil thickness (mm)	0.05	
Foil length (mm)	353	
Effective window size (mm^2)	15 (width) × 25 (height)	

its standard optical system consists of a monolithic Si (111) monochromator (Spieker, Ando & Kamiya, 1984), flat-plate reflection geometry, and a receiving slit as an analyzer. The horizontal parallel slits and vertical parallel slit are set in line on a guide rail, and mounted on the detector arm of the PFPD using clasps as shown in Fig. 1. When the receiving slit is used instead of the horizontal parallel slits, a slit box can be set on a flat plate after the sample chamber (Fig. 1). A scintillation counter is used as a detector. A second scintillation counter is used for monitoring the decay of the incident beam by counting part of the scattering from a Be foil set obliquely between the monochromator and specimen.

3. Experimental and data analysis

The samples used in the present study were National Institute of Standards and Technology Standard Reference Material 674 CeO_2 and milled Brazilian quartz with a particle size of 3–7 μm. The optical axis of the PFPD was first aligned following a standard procedure by using monochromatized radiation with a wavelength of 1.528 Å. The horizontal parallel slits were mounted and their centre axis was set parallel to that of the detector arm. An entrance slit height of 2 mm was chosen for the incident beam. In some measurements a receiving slit with a height of 0.5, 0.2 or 0.1 mm and an entrance slit with the same height as that of the receiving slit were used instead of the horizontal parallel slits for comparison. All results presented in this paper were obtained without using the vertical parallel slit and vacuum path. The profile intensity was step-scanned at step intervals of 0.005–0.02° and a counting time of 2–5 s at each step. The flat specimen was rotated in the plane of the specimen surface during the scan.

Profile intensity data were analyzed using the computer program *PRO-FIT* (Toraya, 1986) for individual profile fitting. Both split-type pseudo-Voigt and split-type Pearson VII functions (Toraya, 1990) were first fitted to find a suitable profile function. The former gave a slightly better fitting and was used as the profile function. Refined least-squares parameters were the background level (b_0), the integrated intensity for the jth peak (I_j), the peak maximum position (T_j), the full-width at half-maximum (FWHM) [$H_j = (H_{Lj} + H_{Hj})/2$], the asymmetry parameter for peak width ($A_j = H_{Lj}/H_{Hj}$), and the η parameters (η_{Lj} and η_{Hjh}), where subscripts L and H represent the parameters of the function solely defined on the low- and high-angle sides, respectively.

4. Results and discussion

4.1. *Diffraction profile*

Fig. 2 shows the two sets of observed and calculated profiles obtained by using HPS1 and HPS2 for three overlapping reflections (122/212, 023/203 and 031/301) from α-SiO_2. The observed profile shapes are well resolved, having a much narrower FWHM for HPS1. The profile asymmetry caused by the axial divergence reaches a minimum at 2θ = 90°. Fig. 3 shows single peak profiles of the (333/511) reflection (2θ = 94.5°) from CeO_2, and their plots on a logarithmic scale so as to exaggerate the tail shape. The profile asymmetry for both HPS1 and HPS2 has the same tendency, *i.e.* slightly higher tails on the high-angle side, and it is more pronounced in the case of HPS1 with a narrower aperture. Moreover, this profile asymmetry did not change even when the horizontal parallel slits were set upside down on the guide rail. Thus, it is primarily due to a cause other than the horizontal parallel slits themselves. One possible source is the incident beam profile from the monolithic monochromator with the groove in a particular shape (Spieker *et al.*, 1984).

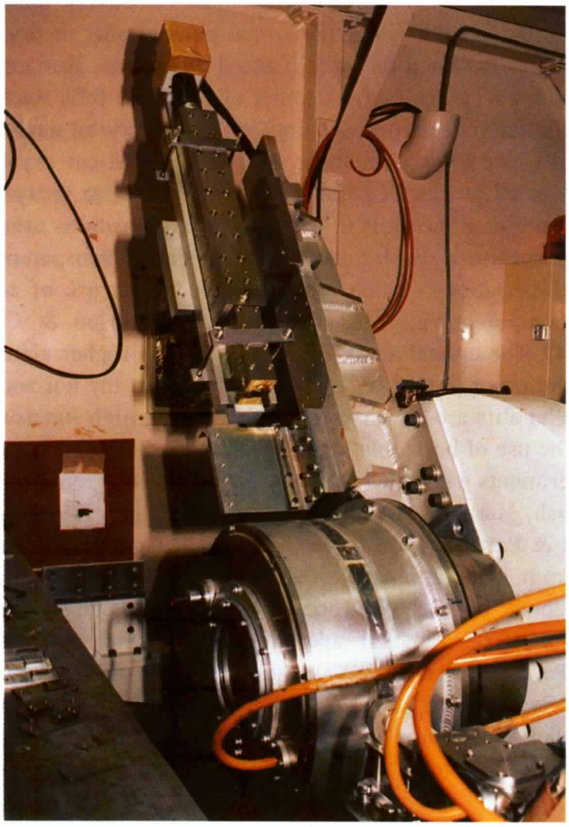

Figure 1
Horizontal and vertical parallel slits mounted on the detector arm of the powder diffractometer PFPD at the BL-4B experimental station at the Photon Factory, Tsukuba.

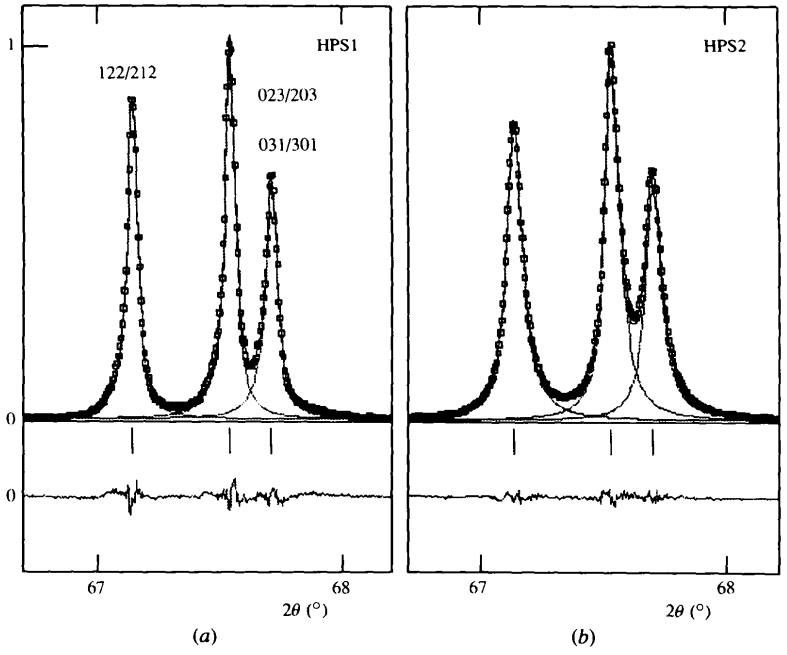

Figure 2
Two sets of observed (squares) and calculated (solid lines) profiles obtained by using (*a*) HPS1, and (*b*) HPS2, for three overlapping reflections from α-SiO_2. Peak maximum positions (short vertical bars) and the difference between the observed and calculated intensities (plot at the bottom of the diagram) are also given.

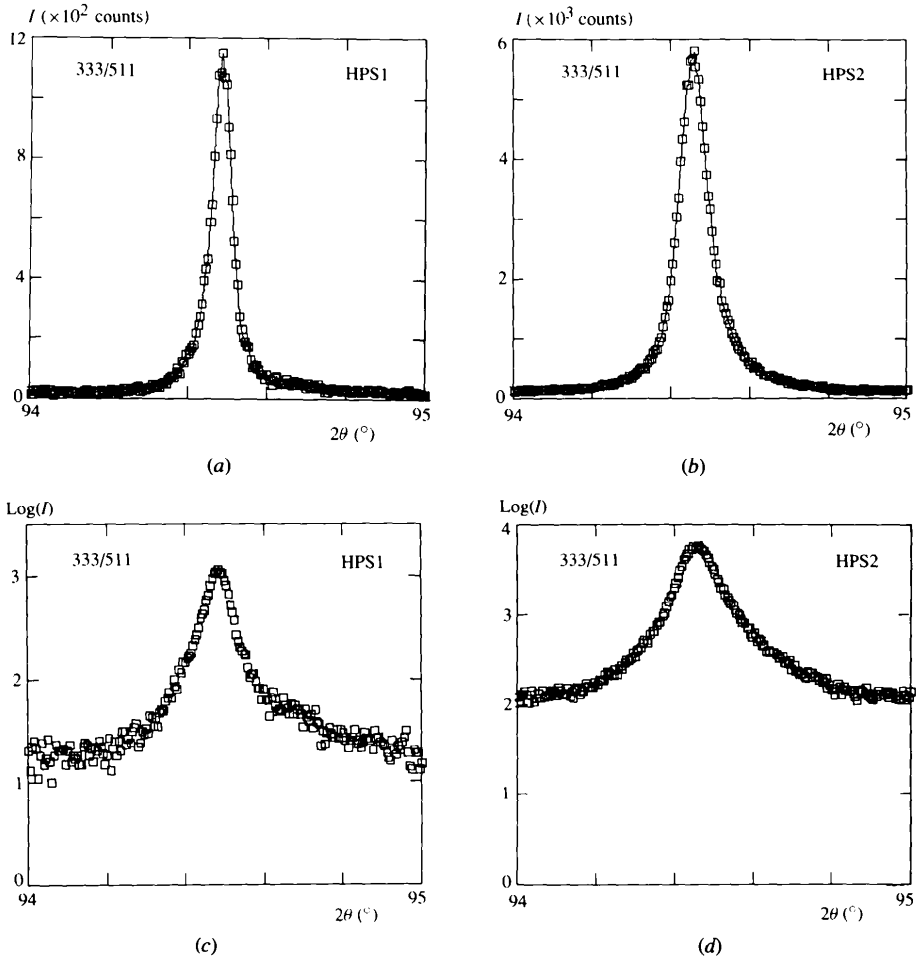

Figure 3
Observed profiles of the (333/511) reflection from CeO_2 obtained by using (*a*) HPS1, and (*b*) HPS2, and their corresponding plots on a logarithmic scale [(*c*) and (*d*)].

Table 2
Comparison of peak maximum intensities and FWHM's in various settings for the slit system.

Slit	Peak maximum intensity (counts s^{-1})	FWHM (°)
HPS1	14223	0.0319
HPS2	24236	0.0582
RS = 0.1 mm	1655	0.0385
RS = 0.2 mm	5199	0.0564
RS = 0.5 mm	15348	0.1153

4.2. *Intensity*

Table 2 gives a comparison of the peak maximum intensity (counts s^{-1}) and the FWHM of the (111) reflection from CeO_2 observed at various slit settings. These intensities were corrected for the decay of the incident beam by using the monitor counts and the background intensity which was subtracted. The X-ray path length between the specimen and counter was 50 cm longer for the horizontal parallel slits than for the receiving slit (Fig. 1). Thus, the intensities obtained using the horizontal parallel slits were also corrected for absorption by air: $\mu_{air} = 0.0103\,cm^{-1}$, and the intensity decreases to about 60% through the air path of 50 cm. The peak maximum intensity obtained using HPS1 is 8.6 times higher than that obtained by a 0.1 mm receiving slit. The intensity will become more than one order of magnitude stronger if the intensities of HPS1 and the receiving slit are compared at the same resolution of 0.032°. The peak maximum intensity is decreased to about one third at each narrowing of the receiving slit from 0.5 to 0.2 mm, and then to 0.1 mm. On the other hand, the intensity is decreased to 59% by replacing HPS2 with HPS1. The relative transmission efficiency of HPS1 against HPS2 is considered quite good if we take into account the ideal value of 84% (Table 1) and the technical difficulty of stacking 167 very long thin foils of stainless steel in parallel.

4.3. *Angular variation of resolution function*

Variations of FWHM with 2θ, observed with HPS1 and HPS2 for the reflections from CeO_2, are shown in Fig. 4. The FWHM for the (200) reflection at $2\theta = 32.810(1)°$ gave the minimum of 0.030 (1)° for HPS1, achieving the primary purpose of the present study. The formulae of Caglioti, Paoletti & Ricci (1958), which were least-squares fitted to the observed data, were: $H(2\theta) = (0.0028\tan^2\theta - 0.0008\tan\theta + 0.0010)^{1/2}$ and $H(2\theta) = (0.0038\tan^2\theta + 0.0012\tan\theta + 0.0027)^{1/2}$ for HPS1 and HPS2, respectively.

4.4. *Alignment of the horizontal parallel slits*

The influence of misalignment of the horizontal parallel slits on the diffracted intensity was examined. The centre axis of the horizontal parallel slits was inclined by an angle φ against the centre axis of the detector arm as shown in Fig. 5. The (111) reflection from CeO_2 was then scanned at various settings of φ. The peak maximum intensities and positions of the (111) reflection are plotted against φ in Figs. 6 and 7, respectively. The intensity does not change with φ (Fig. 6). On the other hand, the Bragg-peak positions are shifted linearly with φ in almost the same gradients for both HPS1 and HPS2 (Fig. 7), and the amount of peak shift is approximately the same as φ. This situation can be

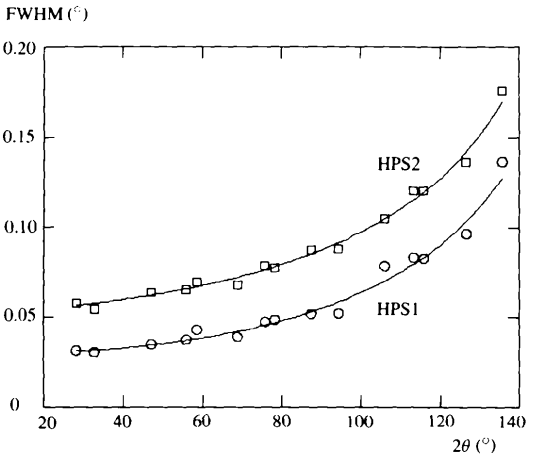

Figure 4
Variations of FWHM with 2θ observed with HPS1 and HPS2 for the reflections from CeO_2.

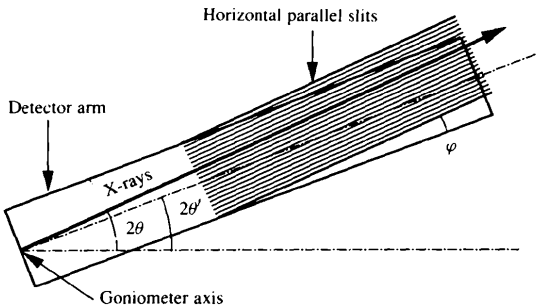

Figure 5
A schematic diagram of the geomety of the detector arm at $2\theta'$ ($= 2\theta - \varphi$). The horizontal parallel slits are inclined by the angle φ against the centre axis of the detector arm and the X-rays are diffracted at 2θ.

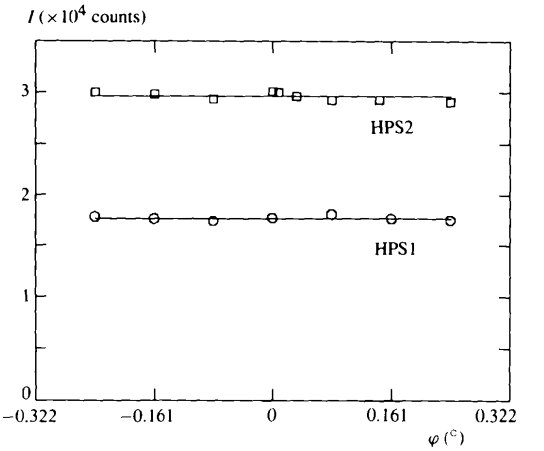

Figure 6
Plots of peak maximum intensities of the (111) reflection from CeO_2 against φ.

explained by the scheme shown in Fig. 5. The horizontal parallel slits are inclined by the angle φ from the centre axis of the detector arm. However, the diffracted beam can pass completely through and between the foils when the detector arm is at the angle $2\theta' = 2\theta - \varphi$. The same situation can occur when a flat crystal or a channel-cut crystal is used as an analyzer. Regarding the alignment of the horizontal parallel slits, two standard steps should be followed: (i) 2θ zero-adjustment of the detector arm using a narrow receiving slit, and (ii) adjustment of the horizontal parallel slits themselves in order to give the maximum intensity at 2θ-zero. Powder diffractometers with parallel-beam optics are considered to be free from X-ray optical correction. The misalignment of the horizontal parallel slits does not affect the diffracted beam intensity, whilst it induces the systematic shift of the Bragg-peak positions.

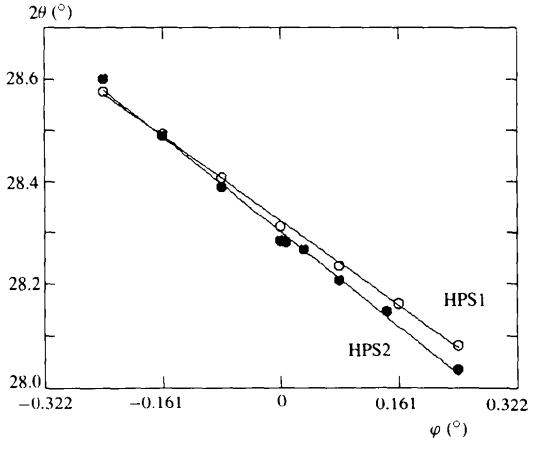

Figure 7
Plots of peak maximum positions of the (111) reflection from CeO_2 against φ.

The present study was financially supported by the JAERI-RIKEN SPring-8 Project Team. The authors are indebted to the staff of the Photon Factory for their help and in making the facilities available. They also thank Dr M. Sakata of Nagoya University for useful suggestions on the construction of horizontal parallel slits.

References

Caglioti, G., Paoletti, A. & Ricci, F. P. (1958). *Nucl. Instrum.* **3**, 223–228.
Cernik, R. J., Murray, P. K., Pattison, P. & Fitch, A. N. (1990). *J. Appl. Cryst.* **23**, 292–296.
Cox, D. E. (1992). *Synchrotron Radiation Crystallography*, pp. 186–254. New York: Academic Press.
Hart, M. (1991). *Mater. Sci. Forum*, **79–82**, 447–454.
Hart, M. & Parrish, W. (1986). *Mater. Sci. Forum*, **9**, 39–46.
Hastings, J. B., Thomlinson, W. & Cox, D. E. (1984). *J. Appl. Cryst.* **17**, 85–95.
Ohno, K., Harada, H., Yamagata, T. & Yamazaki, M. (1991). *Pacific International Congress on X-ray Analytical Methods, Hawaii*. Abstracts, p. 76.
Parrish, W. & Hart, M. (1987). *Z. Kristallogr.* **179**, 161–173.
Parrish, W., Hart, M., Erickson, C. G., Masciocchi, N. & Huang, T. C. (1986). *Adv. X-ray Anal.* **29**, 243–250.
Parrish, W., Hart, M. & Toraya, H. (1990). *Satellite Meeting XVth Congress of the IUCr, Powder Diffraction, Toulouse*. Abstracts, pp. 19–20.
Spieker, P., Ando, M. & Kamiya, N. (1984). *Nucl. Instrum. Methods*, **222**, 196–201.
Takata, M., Kisono, M., Sakata, M. & Sasaki, S. (1993). *Photon Fact. Act. Rep.* **11**, 39.
Toraya, H. (1986). *J Appl. Cryst.* **19**, 440–447.
Toraya, H. (1990). *J. Appl. Cryst.* **23**, 485–491.
Toraya, H., Huang, T. C. & Wu, Y. (1993). *J. Appl. Cryst.* **26**, 774–777.
Uno, R., Ozawa, H., Yamanaka, T., Morikawa, H., Ando, M., Ohsumi, K., Nukui, A., Yukino, K. & Kawasaki, T. (1988). *Aust. J. Phys.* **41**, 133–144.